Transient Effects in Dynamic Modulus Measurement of Silicone Rubber, Part 2: Effect of Mean Strains and Strain History

R. L. Warley,[1] D. L. Feke,[2] I. Manas-Zloczower[3]

[1]*Department of Mechanical Engineering, Penn State Erie, The Behrend College, Erie, Pennsylvania 16563*
[2]*Department of Chemical Engineering, Case Western Reserve University, Cleveland, Ohio 44106*
[3]*Department of Macromolecular Science, Case Western Reserve University, Cleveland, Ohio 44106*

Received 8 March 2006; accepted 13 July 2006
DOI 10.1002/app.25136
Published online in Wiley InterScience (www.interscience.wiley.com).

ABSTRACT: The strain-dependent dynamic storage modulus of a poly(dimethyl-siloxane-*co*-methylvinyl-siloxane-*co*-methylphenyl-siloxane)-based silicone elastomer (PVMQ), which is reinforced with fumed silica and crosslinked with peroxide, is investigated. The time dependence of the dynamic storage modulus on the magnitude of the mean strain at a particular test condition is investigated. The dynamic modulus results are shown to depend on the time of cycling as well as the relative magnitudes of the dynamic and mean strains. The relaxation of the force required to maintain the mean strain is observed to depend on the magnitude of the dynamic strains and the data are shown to be consistent with static stress relaxation experiments in the limit of zero dynamic strain. Recovery of the dynamic modulus from the exposure to higher strain cycling is seen to be facilitated by dynamic cycling with higher cycling strains yielding faster recovery rates. The observed phenomena are interpreted in terms of the role of entanglements in the polymer phase on the dynamic behavior of the elastomer material. © 2007 Wiley Periodicals, Inc. J Appl Polym Sci 104: 2197–2204, 2007

Key words: silicones; elastomers; modulus; relaxation

INTRODUCTION

Recent works[1–4] concerning the dynamic modulus of filled silicone elastomers have suggested that the behavior of the polymer phase plays a significant role in the complex phenomena observed. The role of entanglements in the polymer and the perturbation of the state of entanglement induced by the presence of high surface area particles have been proposed[2,4] to explain the complex behavior of the dynamic modulus of both elastomers and filled thermoplastic polymers above the glass transition. It has been shown[4] that the dynamic storage modulus is time-dependent $G'(\gamma,t)$ and that the stress relaxation modulus $G(\gamma,t)$ depends on strain in much the same way as $G'(\gamma,t)$. It has been proposed[2] that $G'(\gamma,t)$ is determined by the dynamic strain (γ_d) alone when a sinusoidal strain is superposed on a nonzero mean strain (γ_s). Most of the published works[5–9] concerning small dynamic strains superposed on nonzero mean strains were performed in tension deformation with relatively large mean strains. One study[10] conducted using simple shear deformation found no change in G' due to superposed γ_s for small γ_s and a decrease and subsequent partial recovery of G' with larger γ_s. Work has also been done using pure shear[9,11] and biaxial tension[12] geometries with dynamic deformation superposed on static strains.

In addition, a significant decrease in the modulus of filled elastomers occurs when a deformation has previously been applied that exceeds the deformation of the current measurement. This is conventionally known as the Mullins[13] effect. While the Mullins effect is typically thought of in terms of the static response of elastomers, it also affects the dynamic properties. A detailed study[14] of the effect of large shear strain histories on small strain dynamic modulus of carbon black-loaded styrene butadiene rubber has been performed. In addition, dynamic stress softening via repeated strain sweeps in the absence of mean strains has been studied[15] at low deformations.

In the current work, we explore the transient response of a filled silicone elastomer when dynamic moduli are measured in the presence of nonzero mean strains and also when measured after a higher strain cycling history. Our aim is to increase our understanding of the peculiarities of the dynamic moduli of filled elastomers. In addition, it is intended that the information gathered will be useful for specification of meaningful test protocols and for understanding the behavior of elastomers under complex strain histories.

Correspondence to: R. L. Warley (rlw27@psu.edu).

Journal of Applied Polymer Science, Vol. 104, 2197–2204 (2007)

EXPERIMENTAL

Raw materials

The polymer used in all formulations was SE-54 PVMQ silicone gum (GE Silicones, Waterford, NY), which was used as-received without characterization. Typical attributes[16] of the SE-54 gum are $M_n = 3 \times 10^5$, $M_w/M_n = 2.4$, 0.2% by mass vinylmethylsiloxane monomer, 14% by mass diphenylsiloxane monomer. The silica was TS-500 (Cabot Corp. Cab-O-Sil Div., Tuscola, IL), which is a fume process silica (initial BET surface area of 325 m^2/g) that has been treated with hexamethyldisilazane (HMDS) with a resulting N_2 BET surface area of 200 m^2/g. The peroxide was Dicup 40C (Hercules, Wilmington, DE), which is 40% dicumyl peroxide ($C_{18}H_{22}O_2$) dispersed on an inert filler. All materials were used as received.

Masterbatch and compound preparation

The formulations in terms of parts per hundred (phr) of polymer by weight were SE-54, 100; TS-500, various (20–75); Dicup 40C, 1.4.

The peroxide level was chosen to be typical of a practical formulation that might be used to manufacture mechanical goods. The masterbatches were mixed in a 95 L Baker-Perkins sigma blade mixer by adding proportions of the TS-500 to the SE-54 at a mixer temperature of 150°C followed by mixing for 1 h under vacuum after all of the silica was incorporated. The mixing procedures used in this work were typical of what would be used to produce commercial silicone elastomer bases. Three of these 30 kg masterbatches were prepared with silica loadings of 20, 50, and 75 phr of TS-500. These correspond to silica volume fractions (ϕ) of 0.080, 0.179, and 0.247 respectively, assuming a polymer density of 0.96 g/cm^3 and a silica density of 2.2 g/cm^3. Other silica loadings were obtained by blending the masterbatches on a two-roll mill at room temperature. Unless otherwise specified, the silica loading used was $\phi = 0.247$. Total mixing times were 2, 4.5, and 6 h, respectively. The masterbatches were aged for a minimum of 3 weeks (maximum of 10 months) prior to adding peroxide on a two-roll mill at room temperature in ~1 kg batches.

Dynamic modulus measurement

Dynamic property measurement was done using a double lap, simple shear test specimen, which consists of two layers of rubber ~5 mm in thickness bonded to steel supporting members using a silane adhesive during molding and vulcanization. The correction for the bending component of the deformation[17] in this specimen is only 0.52% and is neglected. In this work, all dynamic strains (γ_d) are stated in terms of single strain amplitudes (SSA). Thus the extremes of all dynamic strain cycles are $\gamma_s \pm \gamma_d$.

Prior to molding, the rubber was freshened on a two-roll mill to remove crepe hardening. Identical milling procedures were used throughout this work. The specimens were molded in a six cavity steam heated transfer mold, which fills each side of the specimen with a separate sprue with a gate ~1.6 mm in diameter. Specimens were cured for 20 min at 163°C followed by a 24-h post cure in a circulating air oven at 177°C. The time to fill the mold cavity was of the order of 20 s and the pressure in the transfer pot was ~ 13.5 MPa. The specimens are inserted in a servo-hydraulic test stand by attaching the inner member to a 22 kN load cell through a barrel nut. The outer members are clamped symmetrically to a fixture attached to the hydraulic actuator. The rubber wall thickness is thus constrained to remain constant throughout the test.

The periodic force and displacement time domain signals are decomposed through an FFT algorithm. The complex dynamic modulus (G^*) is calculated as the ratio of the amplitudes of the fundamental force and displacement sinusoids, and δ is defined as the phase angle between the force and displacement fundamental sinusoids. The other dynamic properties are computed from G^* and δ.

The modulus corresponding to the force required to maintain the mean strain $\langle G(\gamma,t)\rangle$ was determined from the zero frequency term of the FFT in the case where the mean strain in the cycle was intentionally nonzero. Unless otherwise specified, each specimen was tested only once and discarded.

RESULTS AND DISCUSSION

Effect of nonzero mean strain

The data generated in this work for combined static and dynamic strain cycles showed somewhat more

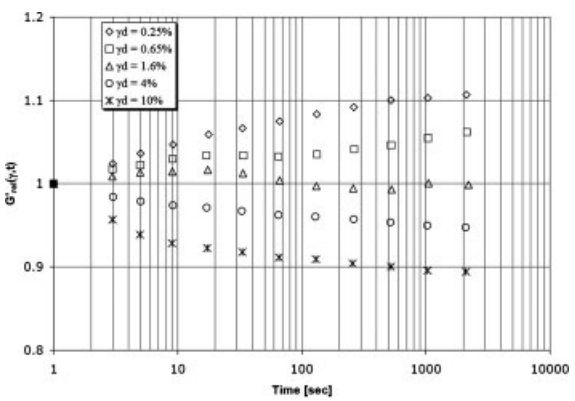

Figure 1 Relative storage modulus $G'_{rel}(\gamma,t)$ as a function of time since mean strain is applied ($\gamma_s = 1.6\%$) for various superposed dynamic strains γ_d (at 23°C and 10 Hz). Dynamic cycling is done in 10 cycle blocks at times indicated.

complicated behavior than previous results.[4] Figure 1 shows results in simple shear wherein a dynamic strain γ_d is superposed on a static (mean) strain γ_s, where γ_s is comparable to γ_d in magnitude. The relative dynamic modulus is defined in this work as $G'_{rel}(\gamma,t) = G'(\gamma,t)/G'(\gamma,1)$, where t is the time (in seconds) since the application of γ_s. The data were plotted as a relative modulus, since the large dependence of $G'(\gamma,t)$ on γ_d would overshadow the time dependence if the data were plotted as the absolute magnitudes. These data were generated by performing blocks of 10 cycles at 10 Hz followed by a delay with no dynamic cycling imposed, while holding γ_s constant. $G'(\gamma,t)$ was extracted from the last eight cycles of the ten cycles performed in each block. As seen in Figure 1, there is a modulus growth when $\gamma_d < \gamma_s$ as opposed to modulus relaxation when $\gamma_d > \gamma_s$. The modulus growth decreases as γ_d increases becoming a modulus relaxation, which increases with increasing γ_d.

The transient behavior of $G'(\gamma,t)$ depends on the details of how the measurement is performed as shown in Figure 2. In all cases, the $G'(\gamma,t)$ measurements were based on the same number of cycles done at the same time intervals, the only difference is what happens to the specimen in the time intervals between measurements. The ''minimal cycling'' data were generated by maintaining γ_s with no extra cycling occurring between the initial measurement and the last measurement. The ''burst cycling'' data were generated by performing blocks of cycles at the time intervals noted, with no dynamic deformation between blocks (same protocol as in Fig. 1). The ''continuous cycling'' data were generated by cycling continuously at γ_d throughout the experiment, with the measurements occurring at the same times and in the same manner as the burst cycling data. Hysteresis heating is negligible for all three cases at the low γ_d used in these experiments. There appears to be an increase in $G'(\gamma,t)$, which is offset by the reduction in $G'(\gamma,t)$ that occurs with cycling of γ_d. The data in Figure 1 are thus qualitatively consistent with the previous finding[4] that the relaxation in $G'(\gamma,t)$ increases as γ_d increases. When $\gamma_d > \gamma_s$, the relaxation of $G'(\gamma,t)$ overcomes the recovery from the application of γ_s. Note that since γ_d is specified in terms of SSA, the specimen is cycled sinusoidally between zero and $2\gamma_d$ when $\gamma_d = \gamma_s$.

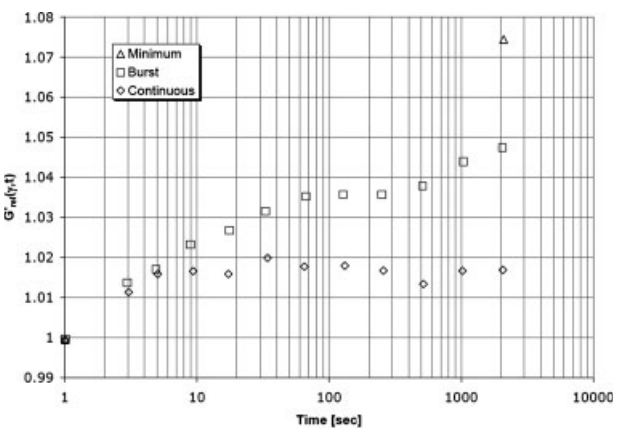

Figure 2 $G'_{rel}(\gamma,t)$ as a function of time since mean strain is applied ($\gamma_s = 1.6\%$) for various modes of cycling $\gamma_d = 0.65\%$ (at 23°C and 10 Hz).

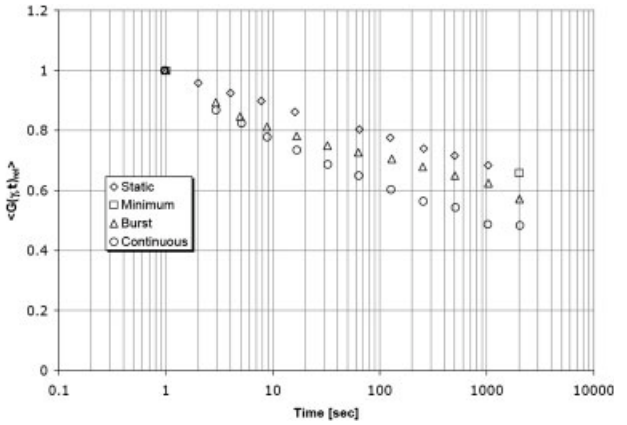

Figure 3 $\langle G(\gamma,t)\rangle_{rel}$ as a function of time since $\gamma_s = 1.6\%$ was applied and mode of cycling $\gamma_d = 0.65\%$ (at 23°C and 10 Hz).

The modulus corresponding to the force required to maintain γ_s ($\langle G(\gamma,t)\rangle$) decreases with time and is a function of the mode of cycling, shown in Figure 3. Superposed on these data is the static stress relaxation [$G(\gamma,t)$] curve[4] at $\gamma_s = 1.6\%$ scaled to the same relative value at zero time. This adjustment was done, since the two different experiments have slightly different timescales. It is apparent that the small strain cycling at $\gamma_d = 0.65\%$ superposed on $\gamma_s = 1.6\%$ is causing significantly greater relaxation of $\langle G(\gamma,t)\rangle$.

A related phenomenon was observed where creep[18] and to a lesser extent stress relaxation[19] were determined to be more extensive if the stress or deformation was applied in a cyclical manner rather than the more common constant application of deformation. In the idealization of linear viscoelastic behavior, a material should obey the Boltzmann superposition principle[20] where the steady loading case would be the lower bound for the stress relaxation experiment. In the data presented here $\gamma_d < \gamma_s$, yet there is a significant enhancement of the stress relaxation of the static component of the stress. This is not simply due to the higher maximum strain, since for these materials the stress relaxation plots are steeper[4] for lower γ_s.

In contrast, the static deformation has little effect on the overall strain dependence of $G'(\gamma,t)$ even in the case where $\gamma_s > \gamma_d$. Figure 4 shows $G'(\gamma)$ for several values of γ_s. These data are consistent with recent findings in simple shear deformation and in contrast with the early work in simple tension. To a first approximation $G'(\gamma)$ depends only on γ_d and not on a combination of γ_s and γ_d over the range investigated.

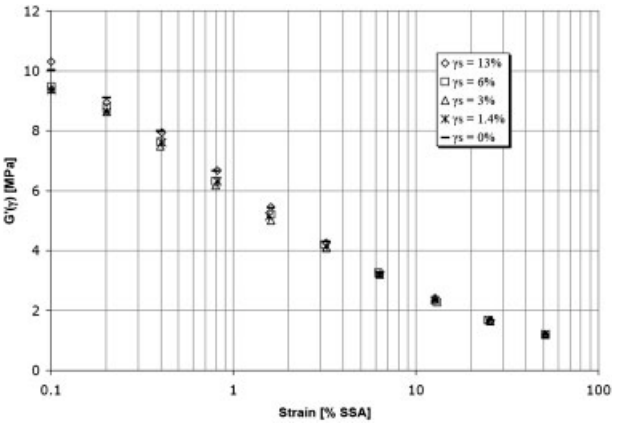

Figure 4 Storage modulus $G'(\gamma)$ as a function of γ_d (at 23°C and 1 Hz). Mean strains γ_s are indicated in figure.

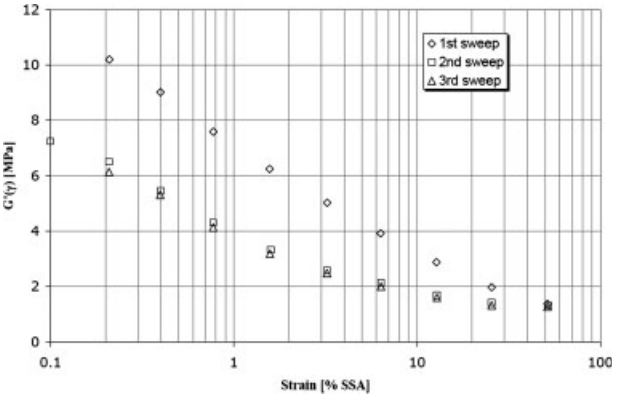

Figure 6 Storage modulus $G'(\gamma)$ as a function of dynamic strain amplitude for three successive increasing strain sweeps at 23°C and 1 Hz.

This is particularly significant since $G(\gamma,t)$ is quite strain-dependent in the region over which γ_s was varied. In fact, the dependence of $G'(\gamma,t)$ on γ_d is quite similar to the dependence of $G(\gamma,t)$ on γ_s.

Cycling at various γ_d superposed on γ_s does significantly affect $\langle G(\gamma,t)\rangle$ however (Fig. 5). This is not too surprising in view of the present data, since for any finite γ_d superposed on γ_s, the maximum strain in the cycle is larger than γ_s, so a reduction in $\langle G(\gamma,t)\rangle$ would be expected. It is interesting to note that the relaxation of $\langle G(\gamma,t)\rangle$ is more pronounced at lower γ_d conditions similar to the behavior of $G(\gamma,t)$ in static stress relaxation. This is the opposite of the dependence of the relaxation of $G'(\gamma,t)$ when γ_d is varied. The static stress relaxation curve corresponding to $\gamma_s = 1.6\%$ is plotted on the same scale (at $\gamma_d = 0$) and indicates that the data are consistent with the static stress relaxation data.[4]

The effect of moderate strain precycling

The first indication of the importance of precycling at larger γ_d appears when successive strain sweeps are performed on the same test specimen (Fig. 6). Three identical sweeps of increasing γ_d with a 10 min delay between tests was used to generate these data. In agreement with prior work,[15] there does not appear to be a significant difference between the second and third sweeps indicating an absence of significant hysteresis heating effects. The reduction of $G'(\gamma)$ due to the repeated sweep is quite pronounced at lower γ_d.

The reduction in $G'(\gamma)$ due to moderate strain precycling depends markedly on the volume fraction of silica in the polymer (Fig. 7). These data were generated by performing a dynamic strain sweep then cycling the specimen to $\gamma_d = 100\%$ for ten cycles followed by a 24 h delay (with the sample removed from the fixture) followed by testing to obtain a strain sweep. The 24 h delay was used to allow thermal and viscoelastic recovery from the moderate strain cycling and was not intended to induce a real recovery from the precycling. Data presented later show that negligible recovery will occur at room temperature in 24 h. Shown in Figure 7 is the ratio of $G'(\gamma)$ measured from the second strain sweep divided by the $G'(\gamma)$

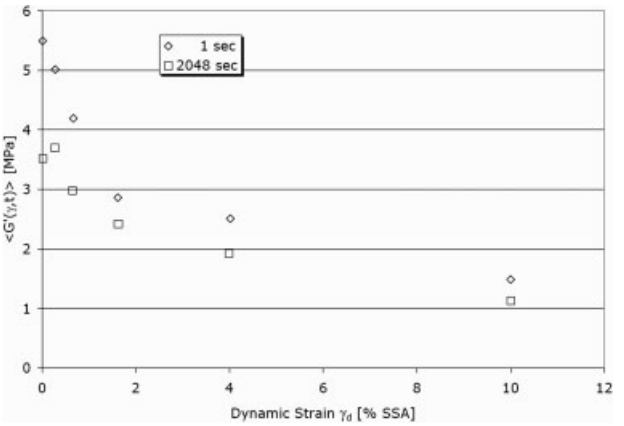

Figure 5 $\langle G(\gamma,t)\rangle_{\text{rel}}$ as a function of superposed dynamic strain and time since $\gamma_s = 1.6\%$ is applied (at 23°C and 1 Hz).

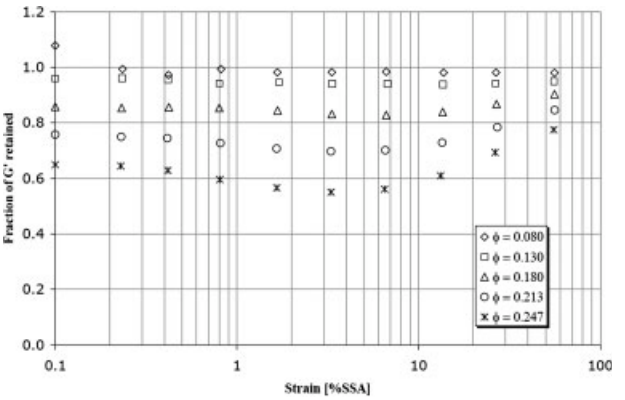

Figure 7 Fraction of storage modulus retained after a ±100% strain preflex at 23°C and 1 Hz as a function of dynamic strain amplitude γ_d and volume fraction of silica ϕ.

measured in the first strain sweep. There is very little reduction in $G'(\gamma)$ for the samples that contain lower volume fractions of silica. The reduction in $G'(\gamma)$ increases as the volume fraction of silica is increased. This is in agreement with the previous work,[13] which found that the greater the reinforcing action of the filler, the greater the softening effect of larger strain cycling.

The effect of moderate strain precycling on the relaxation in $G'(\gamma,t)$ was studied. Figure 8 shows the change in $G'(\gamma,t)$ with time of cycling at γ_d, as a function of the time since a precycling of magnitude $\gamma_c = 100\%$ for 10 cycles is performed. A separate test specimen was used to generate each curve in Figure 8. The change in behavior from a very short rest period to longer rest periods is striking. At short rest periods an increasing transient with cycling time is noted in $G'(\gamma,t)$, but after longer rest times a decreasing transient is present. This type of behavior leads to the interpretation that a recovery process is occurring on the short timescale, which creates a situation in which a relaxation can occur with cycling after enough recovery has taken place.

Recovery from moderate strain cycling

An experiment was performed to investigate the extent and rate of room temperature recovery from moderate strain precycling. The experiment consisted of performing preflex cycles on individual specimens at the indicated number of days prior to the final day, when all of the strain sweeps were performed. This experimental schedule was adopted to remove the influence of any test machine fluctuation over the month duration of the experiment. Each individual point on a given curve was generated from a separate test specimen, and each point on a given curve has a corresponding point on the other two curves that was generated from the same specimen. Figure 9 shows the fractional recovery (G_R) of $G'(\gamma,t)$, defined as the fraction of the change in $G'(\gamma,t)$ (that occurred as a result of the precycling) that has been recovered, versus recovery time. Only at the highest γ_d is the recovery appreciable over a month time period. The lower the test strain, the smaller the extent of recovery is at any given time. No attempt to induce rapid recovery by swelling in solvents or by increasing the temperature was made in this work.

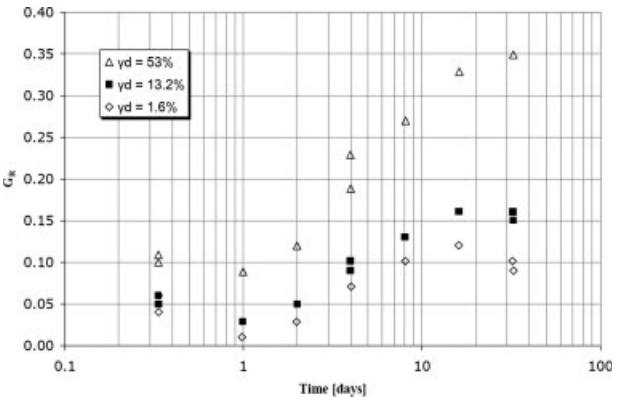

Figure 9 Fractional recovery in $G'(\gamma)$ as a function of strain and rest time since application of ten ±100% preflex cycles at 23°C and 1 Hz.

Figure 10 shows G_R recovery data for samples preflexed to $\gamma_d = 100\%$ and then cycled continuously at the γ_d indicated. The amount of recovery in the very short time period is large compared to the recovery shown in Figure 9, where much longer recovery times were used. The results shown in Figure 11 are even more surprising. Here the data were generated by applying the ten cycle preflex to $\gamma_c = 100\%$ followed by a block of ten cycles to obtain $G'(\gamma,t)$ immediately after the preflex, then allowing time to elapse with the specimen still in the fixture without cycling, then applying another block of ten cycles at the end to mea-

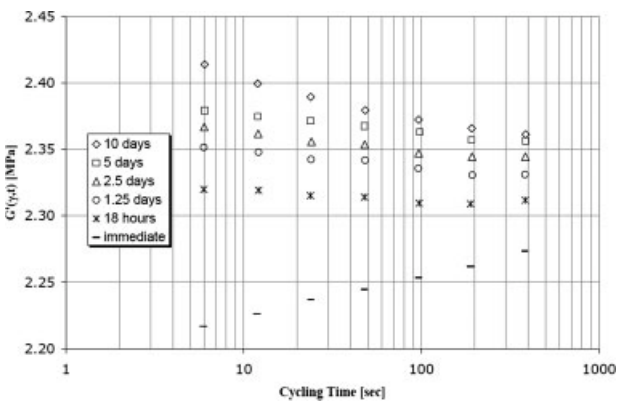

Figure 8 Storage modulus $G'(\gamma,t)$ as a function of cycling time (at 23°C and 1 Hz) and time since application (denoted in figure) of 10 cycles of ±100% strain.

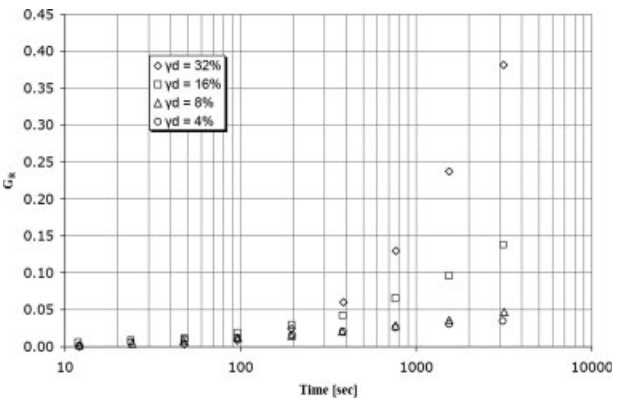

Figure 10 Fractional recovery in $G'(\gamma)$ as a function of time of cycling following ten ±100% precycles at strain indicated at 23°C and 1 Hz. Time zero corresponds to time of completion of tenth cycle of ±100%.

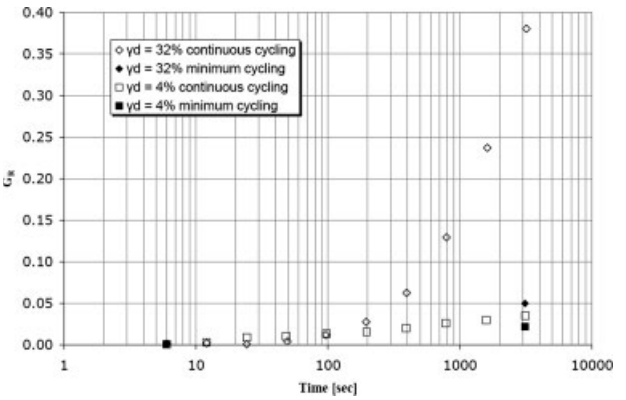

Figure 11 Fractional recovery in $G'(\gamma)$ as a function of time and mode of cycling following ten ±100% precycles at strain indicated at 23°C and 1 Hz. Time zero corresponds to time of completion of tenth cycle of ±100%.

sure the final value of $G'(\gamma,t)$. This was done to remove the variation that is evident in Figure 9, which is due to removal of the test samples from the fixture. The appropriate curves for continuous cycling from Figure 10 are included in Figure 11 for comparison. At $\gamma_d = 32\%$, there is a large difference between the recovery obtained with continuous cycling and the recovery obtained when the sample was allowed to rest between measurements. At $\gamma_d = 4\%$, there is also an enhancement in recovery due to the cycling but to a much smaller degree. The recovery at $\gamma_d = 32\%$ with minimum cycling is only slightly larger than the recovery at $\gamma_d = 4\%$ either with or without cycling. This is consistent with the behavior seen in Figure 9. These data are also consistent with the results shown in Figure 10 in that the resting recovery at $\gamma_d = 32\%$ is larger than the resting recovery at $\gamma_d = 4\%$. The difference between recovery during cycling and the recovery upon standing is quite surprising, particularly since cycling continuously at a given strain without previous cycling at a higher strain is known to cause a relaxation in $G'(\gamma,t)$.

Relaxation in $G'(\gamma,t)$ also occurs if sufficient time is allowed (with no cycling) to elapse between the application of the larger strain cycling (Fig. 8) and the smaller strain cycling. Since hysteresis heating is not a significant factor in the experiments done here, one must conclude that the cycling is facilitating the recovery process.

The recovery process depends on the magnitude of the cycling strain (γ_c) as well as the strain (γ_d) at which $G'(\gamma,t)$ is measured. An experiment was run wherein the recovery of $G'(\gamma_d = 32\%, t)$ for a test sample that had been precycled using ten cycles of ±100% strain was monitored as a function of the cycling γ_c that was done during recovery. This was done to separate the effect of the cycling strain from the strain at which the $G'(\gamma,t)$ is measured. Figure 12 shows the effect of varying γ_c (8, 16, and 32%) on $G'(\gamma_d = 32\%, t)$ during recovery from precycling at 100%. The measurement strain is 32% in all three cases, and γ_c is noted in the figure. Increasing the strain used to cycle the specimen between test blocks speeds the recovery of the $G'(\gamma_d = 32\%, t)$, indicating that it is the higher cycling strain that enhances the rate of recovery rather than recovery simply being faster at higher measurement strains. Superposed on this plot are similar data (from Fig. 10) where the cycling and testing ($\gamma_c = \gamma_d$) were done at the same strains. Note that in these latter cases the fractional recovery is for $G'(\gamma_d = 16\%, t)$ and $G'(\gamma_d = 8\%, t)$. Interestingly, the relative recovery for samples cycled at a low strain but tested at a high strain (open symbols) is quite close to the relative recovery noted when samples are cycled and tested at the same low strain (filled symbols). Thus it appears that it is the γ_c that primarily determines the rate of recovery from precycling rather than the strain at which the modulus is evaluated. These data cannot be compared on a magnitude basis, since the different test strains induce a significant change in base value of $G'(\gamma,t)$. The data for recovery in the absence of any cycling between test segments is shown for comparison.

The role of entanglements in the observed behavior

These phenomena can be qualitatively interpreted in terms of entanglements in the polymer phase. Entanglements are often thought of in terms of extra crosslinks due to intermolecular trapping of looped chains without a covalent bond being required at the junction. The idea of an unknotted entanglement in elastomers was developed in detail[21] and was used to demonstrate that this type of entanglement can be shown to exhibit some of the properties of a polymer reinforced with particulate fillers. The key idea is that the entanglement is not locked in place by knotting but is

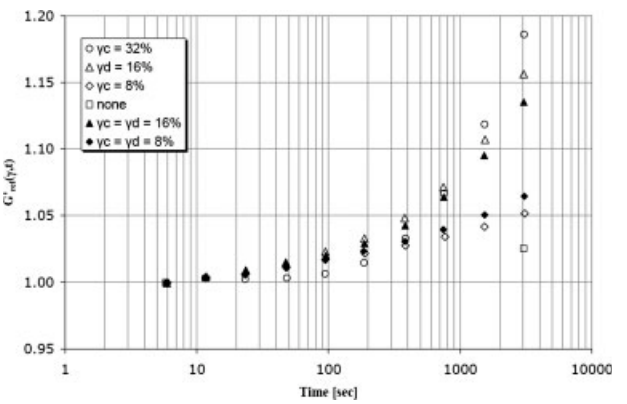

Figure 12 $G'_{rel}(\gamma,t)$ versus time since completion of ten ±100% precycles as a function of strain of cycling γ_c for measurement strains γ_d of 32, 16, and 8% SSA at 23°C and 1 Hz.

merely a tangle prevented from disengaging by other network features in the neighborhood of the tangle.

This can be envisioned as a tangled strand of yarn where the tangling cannot be undone by simply pulling on the ends but can be undone without using the ends of the yarn by tedious manipulation of the trapped loops along the strand. Many ''knots'' in tangled yarn or string are actually unknotted, since they can be undone without involving the ends of the strand. The ''knot'' formed by simply pulling on the ends of the strand forms because of topological constraints and not a true knot.

Entanglements envisioned to be persistent due to tangling, which is unknotted, would be expected to have a long timescale for disentanglement, since disentanglement potentially requires cooperative movement of other chain segments in the vicinity of the tangle.

The importance of this type of entanglement might significantly increase when particulate fillers are added to the polymer, since the polymer is known to strongly adsorb on the surface of the silica and form bound rubber. Since a linear molecule has exactly two ends and many units in between, it is much more likely that an adsorption will occur along the chain length rather than with a terminal unit. If the adsorption of a chain on the surface is strong and persistent, then there will be two ''chains'' emanating from the adsorption point on the surface of the particle. A chain is considered in this context to be one strand of linear polymer protruding from the surface of the silica. The average molecular weight of these chains will be less than the average molecular weight of the polymer. This discussion is considerably simplified, since a complex multiple attachment mechanism[22] was required to explain data on the adsorption of PDMS on silica. If there are multiple attachments along an adsorbed chain then one would expect dangling loops of polymer that would appear as a chain of lower molecular weight that is adsorbed on both ends to the same particle. In this case, there are multiple opportunities for entanglements to occur with a single molecule adsorbed to the surface.

When γ_s is imposed on the sample, it is envisioned that some disentanglement will occur since $G(\gamma,t)$ decreases with γ_s. New entanglements are free to form in the mean deformed state, however. These entanglements can contribute to the strain energy for any dynamic strain superposed on the static deformation. The time dependence of $G'(\gamma,t)$ superposed on a mean strain (Fig. 1) is consistent with this idea. The dependence on the manner in which cycling is done (Fig. 2) can be thought of as a consequence of two competing processes going on simultaneously, namely a reduction in $G'(\gamma,t)$ due to the dynamic cycling and an increase in $G'(\gamma,t)$ due to newly formed entanglements. The more time spent cycling superposed on γ_s, the more the disentanglement process will occur relative to the re-entanglement from the mean deformed state. This also is consistent with a net increase in $G'(\gamma,t)$ when $\gamma_s > \gamma_d$ and a decrease when $\gamma_s < \gamma_d$ (Fig. 1). Since only those entanglements that would not be disentangled by the γ_d will form, the increase in $G'(\gamma,t)$ will be larger for $\gamma_d < \gamma_s$.

The enhancement of the relaxation of $\langle G(\gamma,t)\rangle$ when dynamic cycling is superposed on γ_s (Fig. 3) is analogous to the phenomenon whereby a stress applied cyclically showed more creep than a static application.[18] This was also shown to be true but to a lesser degree in the case of cyclically applied deformation.[19] Since in these data $\gamma_s > \gamma_d$, which represents a deformation that is partially static and partially cyclical, it seems that the deformation need not be totally removed for enhancement of stress relaxation to take place. The time required to apply a static deformation will certainly be shorter than the time for all of the multiply constrained entanglements to release. Thus some entanglements that have the potential to be released will be trapped topologically within the network even though the chains are in random thermal motion. Upon each application of a deformation, there is a probability that a given entanglement will release before it becomes trapped due to local network conditions. If the test sample deformation is released and then repeated, any trapped entanglements have a new chance to release upon application of the deformation, since the topological conditions in the neighborhood of the tangle would have changed, both because of the random thermal motions and due to any disentanglement that occurred on previous deformation cycles.

Since $G(\gamma,t)$ exhibits a dependence on γ_s similar to the dependence of $G'(\gamma,t)$ on γ_d and the dependence appears in one cycle yet decreases with time under deformation, one would initially expect that the presence of γ_s would cause a reduction in $G'(\gamma,t)$ for all $\gamma_s > \gamma_d$. Since the dependence of $G(\gamma,t)$ on γ_s appears with a single application of γ_s the network is able to respond to the strain during the application of the deformation. The value of $G'(\gamma,t)$ will depend on the number of entanglements that are released due to γ_d, since the initial drop due to γ_s has already occurred. In this way, it is possible for $G'(\gamma,t)$ to depend on γ_d yet be independent of γ_s, and to have $G(\gamma,t)$ depend on γ_s and on a superposed γ_d.

If we presume that the effect of moderate strain precycling causes disentanglement in the polymer phase and recovery is accomplished by a re-entanglement mechanism, then it is reasonable to envision that the modulus at larger strains relative to the preflex strain will be affected more than the modulus at lower strains. If a chain that remains entangled at a given dynamic strain, and thus acts as a crosslink, is pulled free by the application of a larger strain, then the distance the chain has to diffuse back into the entangled

chain network to act as a crosslink is larger for lower strains.

The dependence of the recovery at a given measurement strain is much more pronounced if the strain is cycled during recovery (Fig. 11). Not all paths a chain may take in the re-entanglement process will lead to a constrained entanglement that will act as a crosslink. The cycling provides an extra source of molecular motion other than normal thermal motion in the polymer. The combination of random thermal motion and the motion of the matrix combine to give the chain more opportunity to find a path to a persistent entanglement. This concept hinges on a potentially persistent entanglement being locked-in during a strain cycle, if the topology is right for a persistent entanglement to form.

Since the recovery is more pronounced for cycling strains closer to the strain at which $G'(\gamma,t)$ is measured, the recovery process must be more dependent on the motion of the matrix than on the energy storage capacity of the forming entanglements. At larger cycling strains it is obvious that the matrix motion will be greater, but in order for an entanglement to persist for a given cycle, it will have to be capable of withstanding more strain energy as the cycling strain is increased, since the difference between the cycling strain and the measuring strain increases as the cycling strain decreases.

CONCLUSIONS

The results presented in this work are consistent with the idea that entanglements present due to the adsorption of a proportion of the polymer on the highly active silica surface are important in the dynamic mechanical response of filled elastomers. There are transient effects in both the dynamic and static components of the modulus when dynamic strains are superposed on a static strain. These effects appear to be a combination of a reduction in $G'(\gamma,t)$ due to cycling and an increase in $G'(\gamma,t)$ due to recovery from the application of the static strain. Cycling of a small dynamic strain on a static strain is seen to increase the stress relaxation of the static component. Recovery from cycling at higher strains is seen to be markedly accelerated by the presence of dynamic cycling with the recovery being significantly faster for higher cycling strains.

Practical implications for the design of testing protocols are apparent from these findings. Consideration of the transient effects is quite important if dynamic modulus information is needed in a very precise manner. Just as the response of reinforced elastomers in the displacement domain is quite complex, the response in the time domain is similarly perplexing. Any attempt at generation of a constitutive relation will need to include the time domain effects if it is to model the behavior accurately. Further work is required to more fully characterize the behavior of these materials toward dynamic characterization experiments.

The authors thank Lord Corp. (Cary, NC) for their support of this work. Gary Jackson deserves special thanks for his meticulous execution of the dynamic property measurements.

References

1. Funt, J. M. Rubber Chem Technol 1988, 61, 842.
2. Sternstein, S. S.; Zhu, A. J. Macromolecules 2002, 35, 7262.
3. Warley, R. L.; Feke, D. L.; Manas-Zloczower, I. J Appl Polym Sci 2005, 97, 1504.
4. Warley, R. L.; Feke, D. L.; Manas-Zloczower, I. J Appl Polym Sci 2005, 98, 1001.
5. Dutta, N. K.; Tripathy, D. K. Polym Test 1990, 9, 3.
6. Voet, A.; Morawski, J. C. Rubber Chem Technol 1974, 47, 765.
7. Namboodiri, C. S. S.; Tripathy, D. K. J Appl Polym Sci 1994, 53, 877.
8. Meinecke, E. A.; Maksin, S. Rubber Chem Technol 1981, 54, 857.
9. Sullivan, J. L.; Demery, V. C. J Polym Sci Polym Phys Ed 1982, 20 2083.
10. Isono, Y.; Ferry, J. D. Rubber Chem Technol 1984, 57, 925.
11. Sullivan, J. L. J Appl Polym Sci 1983, 28 1993.
12. Sullivan, J. L. J Polym Sci Part B: Polym Phys 1986, 24, 161.
13. Mullins, L. Rubber Chem Technol 1969, 42, 339.
14. Arai, K.; Ferry, J. D. Rubber Chem Technol 1986, 59, 241.
15. Wang, M.-J.; Patterson, W. J.; Ouyang, G. B. Kautchuk und Gummi Kunststoffe 1998, 51, 106.
16. NTIS Report UCID-19644. Lawrence Livermore National Laboratory, Livermore, CA, January 1983.
17. Rivlin, R. S.; Saunders, D. W. Trans Inst Rubber Ind 1949, 24, 296.
18. Derham, C. J.; Thomas, A. G. Rubber Chem Technol 1977, 50, 397.
19. McKenna, G. B.; Zapas, L. J. Rubber Chem Technol 1981, 54, 718.
20. Boltzmann, L. Pogg Ann Phys Chem 1876, 7, 624.
21. MacArthur, A. J. Ph.D. Dissertation, University of Akron, Akron, OH, 1985.
22. Cohen-Addad, J. P.; Roby, C.; Sauviat, M. Polymer 1985, 26, 1231.